Acta Biochimica Polonica

Vol. 48 No. 2/2001

511–523

QUARTERLY

Effect of Mg^{2+} on kinetics of oxidation of pyrimidines in duplex DNA by potassium permanganate[✪]

Tomasz £oziński and Kazimierz L. Wierzchowski[½]

Institute of Biochemistry and Biophysics, Polish Academy of Sciences, Warszawa, Poland

Received: 22 May, 2001; accepted: 30 May, 2001

Key words: pDS3 plasmid DNA, quantitative permanganate footprinting, oxidation of pyrimidines, thymine glycol, rate constant of oxidation, magnesium ions

Potassium permanganate oxidation of pyrimidine bases is often used to probe single-stranded regions in functional DNA–protein complexes. However, so far reactivity of these bases in double-stranded DNA has not been studied quantitatively. We have investigated the kinetics of oxidation of pyrimidines in supercoiled pDS3 plasmid dsDNA by quantitative $KMnO_4$ footprinting, in connection with parallel studies on the effect of Mg^{2+} on kinetics of oxidation of individual thymines in the single-stranded region of the open transcription complex of *Escherichia coli* RNA polymerase at a cognate Pa promoter contained in this plasmid. Rate constants of oxidation for pyrimidines, k_j, in selected regions of pDS3 DNA, including Pa promoter, were determined under single-hit reaction conditions in the absence and presence of 10 mM $MgCl_2$. Their values appeared to be sequence-dependent and were: (i) the largest for Ts in 5′TA3′ and 5′TC3′ steps, while 2–4 times smaller for 5′-adjacent ones in TT(A,G,C) and TTT(A) runs, (ii) for Cs in 5′TC3′ steps 2–4 fold smaller than for adjacent Ts, and (iii) in the presence of Mg^{2+} generally larger by a sequence-dependent factor: in 5′TC3′ steps of about 2 and 4 for Ts and Cs, respectively, in 5′TA3′ steps of TTA and TTTA sequences for 3′-terminal Ts of about 3, while for their 5′-neighbors of a distinctly smaller value of about 2. Comparison of k_j data for corresponding Ts located between +1 and –10 regions of Pa promoter in dsDNA and in ssDNA form in the open transcription complex, reported elsewhere, demonstrates that reactivity of pyrimidines in dsDNA is by 2–3 orders of magnitude smaller. The effect of Mg^{2+} in dsDNA is interpreted in terms of electrostatic barrier to diffusion of MnO_4^- on DNA surface, which is lowered by diffusive binding of these ions to backbone phosphates, involving also sequence-specific contacts with bases in the minor and major grooves of B-DNA.

[✪]This work was partly supported by the State Committee for Scientific Research (KBN, Poland) grant 6 P203 024 06 to KLW.

[½]Corresponding author: Kazimierz L. Wierzchowski, Institute of Biochemistry and Biophysics, Polish Academy of Sciences, A. Pawiñskiego 5a, 02-106 Warszawa, Poland; tel: (48 22) 658 4729; fax: (48 22) 658 4636; e-mail address: klw@ibb.waw.pl

Potassium permanganate reacts with DNA *via* oxidation of 5,6 double bonds of pyrimidines, primarily of thymine, to corresponding glycols [1, 2]. Since the 5,6 double bond of pyrimidine ring is attacked either from above or below the plane of the base, particularly efficient oxidation of pyrimidine residues has been observed when stacking interactions between base pairs in double-stranded DNA were distorted thermally [3] or by intercalation of polycyclic aromatic molecules [4], or were absent as in single-stranded DNA domains formed in complexes with specific proteins [5] or with polyamide nucleic acids [6, 7]. Therefore, $KMnO_4$ has been widely used as the chemical probe for detection of single-stranded regions of DNA in open transcription complexes *in vitro* and *in vivo* [5, 8].

We have recently examined $KMnO_4$ oxidation of the open transcription complex formed at the synthetic consensus-like *Escherichia coli* promoter Pa carried on pDS3 plasmid [9] by the cognate RNA polymerase, in order to quantify the effect of Mg^{2+} ions on the rate constant of oxidation of individual T residues within the transcription bubble. It has been found that Mg^{2+} ions when bound to the complex at 10 mM concentration increase the rate of oxidation of all T residues within the transcription bubble and that the magnitude of this effect strongly depends on location of Ts with respect to the transcription start site: reactivity of Ts located close to this site became 2–3 fold higher than that of those lying more distantly therefrom.

In this connection, it was of interest to determine the reactivity of pyrimidine bases towards $KMnO_4$ in free pDS3 plasmid DNA, including Pa promoter, and the effect of Mg^{2+} ions thereon in order to compare the reactivity of thymines in dsDNA with that within the transcription bubble in which the DNA strands are separated and embedded in protein matrix of $E\sigma^{70}$. To our best knowledge, the reactivity of pyrimidine bases in dsDNA with $KMnO_4$ has been studied only semi-quantitatively [3], with the aim to elucidate the effect of A_n bending tracts on local DNA structure. Therefore, evaluation of oxidizability of pyrimidine bases in dsDNA seemed to be also of a more general interest. Here we report the results of this study. Quantitative analysis of footprints of the studied dsDNA obtained at a number of the oxidant doses allowed determination of the reactivity rate constants of pyrimidines in selected DNA fragments differing in base sequence in the absence and presence of Mg^{2+} ions. We show that reactivity of pyrimidine residues in dsDNA is sequence-dependent, by 2–3 orders of magnitude lower than that found for T residues in single-stranded DNA within the transcription bubble [9], and, in the presence of Mg^{2+}, generally increased by a sequence-dependent factor of 2–4. These findings indicate that enhancement by Mg^{2+} ions of the reactivity of pyrimidines in dsDNA towards MnO_4^- attack is generally electrostatic in nature but its variation parallels sequence-dependent hetereogeneity of dsDNA structure and dynamics as well as base-specific binding of hydrated ions in DNA grooves.

MATERIALS AND METHODS

Materials. The supercoiled pDS3 plasmid DNA (4081 bp) containing promoter Pa was obtained and purified as described earlier [10, 11]. Klenow fragment of DNA polymerase I and polynucleotide kinase were from Boehringer (Mannheim), and [γ-^{32}P]ATP from Amersham. A DNA primer, Pr(nt), complementary to the non-template DNA strand from position +78 to +99 relative to the transcription start point +1 of the Pa promoter, was synthesized by the solid phase phosphoramidite method and purified by denaturing PAGE followed by DEAE-Sephacel column chromatography and ethanol precipitation. The 5′-end of Pr(nt) was phosphorylated in the presence of a 2-fold molar excess of

[γ-^{32}P]ATP by polynucleotide kinase. All other chemicals were molecular biology grade products.

$KMnO_4$ footprinting. Oxidation of pyrimidines in dsDNA by $KMnO_4$ as a function of the oxidant dose, and detection of the oxidation products by the primer extension reaction with use of the Klenow enzyme were performed according to [8]. The procedure applied was exactly the same as used for footprinting of transcription open complex at the Pa promoter on pDS3 plasmid [9], except that higher oxidant doses were used. Reactions were carried at following final $KMnO_4$ concentrations: 0.5, 1, 2, 4 and 8 mM, for 4 min at 37°C. Footprints of one DNA strand, corresponding to nontemplate strand of the Pa promoter, were analyzed. Each footprinting reaction was duplicated and products of each reaction twice separated in parallel by PAGE, so that on the whole four footprints at each oxidant concentration were obtained and analyzed, as described below.

Phosphorimager analysis and quantification of band intensities. Images of footprints were obtained with the use of a Molecular Dynamics Phosphorimager. Integrated intensities of arbitrarily selected groups of bands, marked as blocks 1 to 3 in Fig. 1, were obtained by the volume integration method of the "ImageQuant" software, using as a background an area of the gel without radioactivity (outside the lanes). These intensities were used to calculate corresponding fractions of the oxidized DNA corrected for spontaneous termination of primer extension at non-oxidized bases, the extent of which was evaluated from the control lane with non-oxidized DNA. Intensities of resolved DNA bands and groups thereof in blocks 2 and 3, assigned to particular oxidized bases, were evaluated using the area integration option of the ImageQuant. The intensity profiles thus obtained for partially overlapping bands were deconvoluted into individual Gaussian components with help of ORIGIN 4.0 software under assumption of a constant band halfwidth.

RESULTS AND DISCUSSION

Free pDS3 plasmid dsDNA bearing Pa promoter was exposed to a number of $KMnO_4$ concentrations (from 0.5 to 8 mM) for t = 4 min in a buffer containing 100 mM KCl, in the absence and presence of 10 mM $MgCl_2$. The oxidized bases were detected by the primer extension reaction carried out on the nontemplate DNA strand with the use of the 5′-^{32}P-end-labeled Pr(nt) primer and Klenow fragment of DNA polymerase I. The reaction products terminated at the first oxidized base encountered by the enzyme (or at a preceding one when the glycol form of the oxidized base was hydrolyzed to urea [12]) were separated on DNA sequencing gel. An autoradiogram of a representative footprinting gel is shown in Fig. 1, panel (a). For determination of reactivity of pyrimidines in dsDNA, the footprints were divided into three blocks and two of them which contained well resolved bands of shortest DNA fragments (up to 140 bp) were analyzed: block b2 comprising the whole Pa promoter sequence rich in AT base pairs, and b3 containing equal amounts of AT and GC base pairs (cf. Fig. 1, panel b). The bands were assigned to particular bases in sequence shown along the rightmost lane of the footprinting gel. The assignment was made on the basis of known sequence of pDS3 and characteristic pattern of intense DNA bands within the Pa promoter sequence due to oxidized Ts in 5′TA3′ steps, known to be highly reactive [3].

The integrated intensities of most DNA bands at the low oxidant doses applied were rather small as compared with those of the analyzed blocks of the footprinting gels, hence it was not possible to determine corresponding fractions of oxidized bases with a reasonable accuracy. Therefore, first fractions of oxidized DNA in the analyzed blocks at moderate oxidant doses were determined by volume integration, and then contributions from bands due to particular oxidized pyrimidines evaluted. The latter were determined by area

integration followed by deconvolution into gaussian components of the intensity profiles thus obtained.

nied by a weaker band, cf. for instance those assigned to T+3, T–2 and T–16 in 5′TG3′ and 5′TA3′ sequence steps, due to termination of

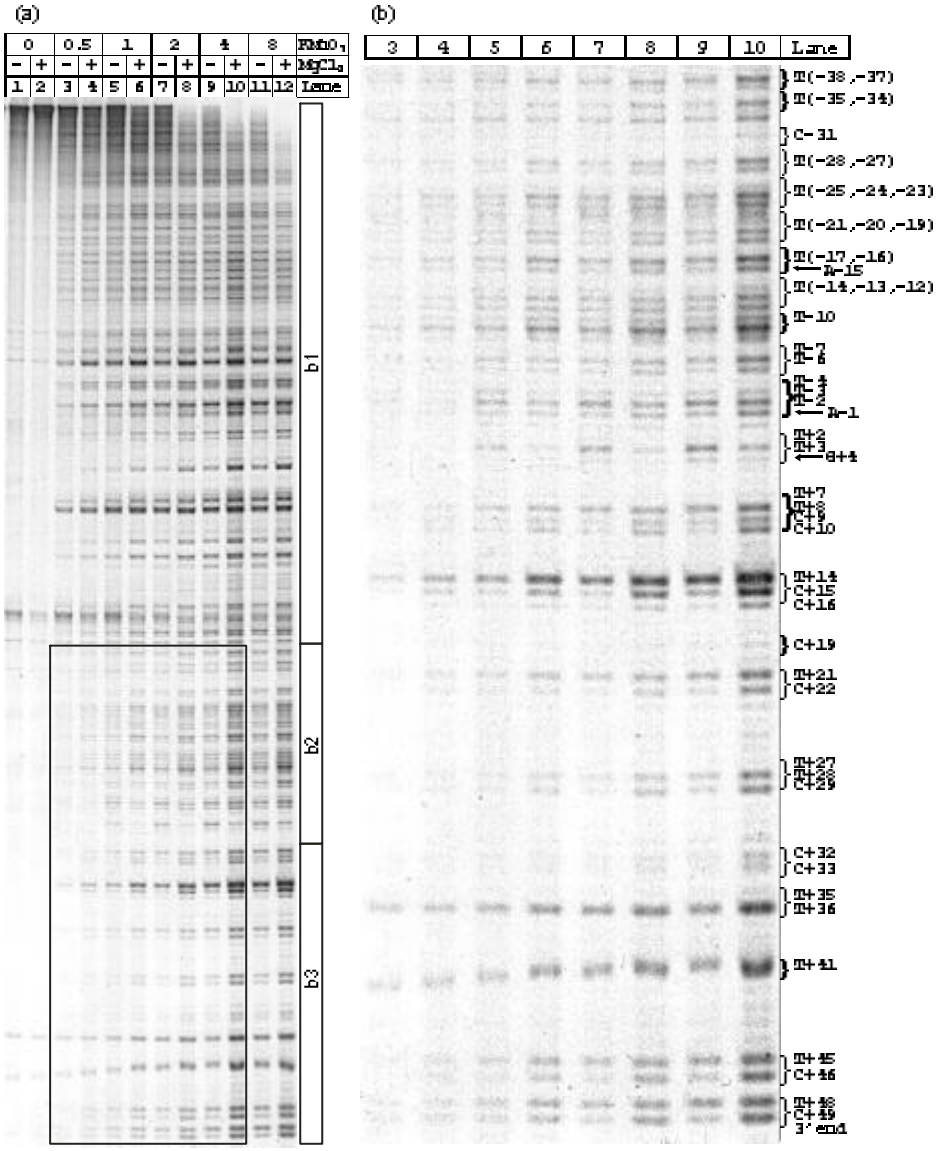

Figure 1. Autoradiogram of $KMnO_4$ footprinting gel of a fragment of pDS3 plasmid dsDNA containing cloned Pa promoter.

$KMnO_4$ concentration (in mM) indicated at the top for pairs of lanes, in the absence (lanes marked "–") and presence of 10 mM $MgCl_2$ (lanes marked "+"). PAGE resolved ^{32}P-end-labeled DNA fragments are products of the primer extension reaction carried on nontemplate pDS3 DNA strand, with respect to the promoter Pa. Along the right side of panel (a) are indicated blocks of bands (b1–b3) used for analysis, in panel (b) is shown an enlarged footprint of b2+b3, along its right side groups of bands are assigned to oxidized pyrimidines in the sequences listed in Fig. 3; arrows mark purines at which primer extension reaction was terminated when the 5′adjacent oxidized thymine was in form of an ureaderiva tive (see text).

Inspection of the footprints indicates that some bands, assigned to oxidized thymines flanked from 3′ side by a purine, are accompa-

the primer extension reaction one base before an oxidized pyrimidine when the glycol form of the latter is hydrolyzed to an ureidoderiva-

tive [12] during denaturation of oxidized DNA under alkaline conditions. Therefore, in evaluation of intensities of the bands along a lane such doubling of bands was taken into the account. In the case when an oxidized pyrimidine was 3′-flanked by a purine, intensities of the two bands were added; when the 3′-flanking base was a pyrimidine, first a contribution due to the ureido form to the band intensity of the latter base was subtracted (it was evaluated assuming the same ratio between the glycol and ureido forms as measured in the former case) and the remaining intensity attributed to the oxidized flanking base.

Fractions of oxidized DNA in each block were determined relative to the integrated intensity of a part of a given lane contained between the top of b1 and the bottom end of the analyzed block, to avoid complications connected with quantification of the footprints in the multiple-hit range of the oxidant doses [13]. Fractions f_i (i = 2, 3), determined at $[Mg^{2+}] = 0$ and $[Mg^{2+}] = 10$ mM, are plotted in Fig. 2 (panels a and b) against corresponding oxidant dose x, i.e. a product of oxidant concentration c (in M), and time of exposure *t* (in s). For some most reactive Ts in each block it was possible to determine corresponding

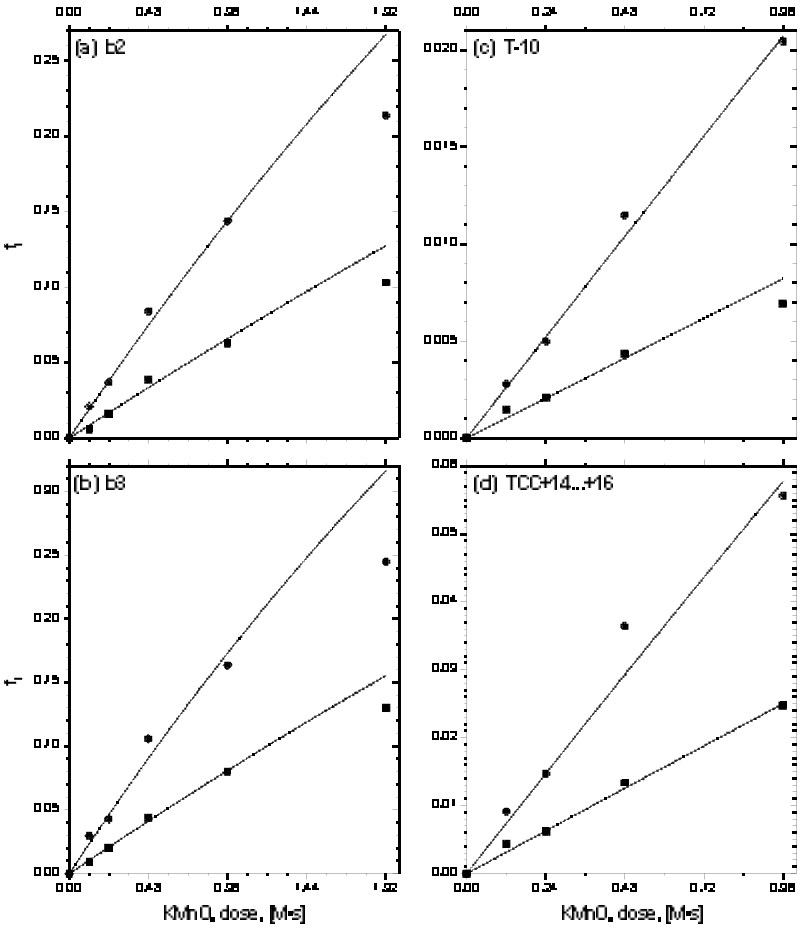

Figure 2. Plots of fractions f_i, of oxidized pDS3 dsDNA in blocks b2 and b3, and of oxidized T–10 and TCC(+14,+15,+16), as a function of $KMnO_4$ dose (x) in the absence (solid squares) and in the presence (solid circles) of 10 mM $MgCl_2$.

Data points, f(x), were obtained by quantification of footprints (exemplified in Fig. 1) as described in Materials and Methods; the calculated mean standard deviation (n = 4) varied in the range of 10–30 per cent relative to the f(x) value. The solid lines drawn through the experimental data points are the calculated fitting functions found by non-linear weighted least squares analysis of the experimental data from the $KMnO_4$ dose (x) range of 0–0.96 Ms according to eqn. 1. Values of the fitted k_i and k_j parameters (in $[M^{-1}s^{-1}]$): $k_2 = 0.071$, $k_{2,Mg} = 0.162$, $k_3 = 0.088$, $k_{3,Mg} = 0.198$, $k_{T-10} = 0.0086$, $k_{T-10,Mg} = 0.0218$, $k_{T+14} = 0.024$, $k_{T+14,Mg} = 0.053$ (the latter two values were corrected for the presence of C+15 and C+16 in the TCC sequence).

fractions f_j of oxidized DNA in the whole range of the oxidant doses. Those for T–10 of b2 and TCC(+14...+16) of b3 are similarly plotted in panels c and d of Fig. 2.

To determine reactivity rate constants, a single exponential function (eqn. 1) was fitted to the f_i and f_j data from the single-hit range of oxidant doses up to x = 1 Ms, conforming to the proposed criteria [13]:

$$f = 1-\exp(-kx) \quad (1),$$

where k is $k_i = \Sigma k_j$, a sum taken over all individual reactivity pseudo first-order rate constants k_j of the bases contained within a given DNA fragment, or k_j when $f = f_j$. The fits proved to be satisfactory for all the $f_i(x)$ and $f_j(x)$ data (cf. lines drawn through experimental data points in Fig. 2). Values of the fitted parameters are listed in the legend to Fig. 2.

Values of k_j for particular bases in a given block were then calculated as products of k_i and f_j/f_i, i.e. contributions to f_i of fractions f_j assigned to each oxidized pyrimidine. The thus obtained k_j values for T+14 and T–10 proved to be similar, within an experimental error of approx. 15%, to those determined independently by fitting eqn. 1 to the respective f_j (x) data for these two bases. This observation validated the analytical approach applied. The reactivity profiles for the analyzed DNA blocks at ± Mg^{2+} conditions are shown as column plots in Fig. 3 (panels a and b), along with the ratio of $k_{j,Mg}/k_j$, taken as a measure of the influence of Mg^{2+} on k_j.

Analysis of the k_j and $k_{j,Mg}$ data indicates that the reactivity of pyrimidines with $KMnO_4$ (i) depends on DNA sequence and (ii) in the presence of 10 mM $MgCl_2$ is larger also by a sequence-dependent factor.

In the b2 fragment, made for the most part of AT base-pairs distributed in a number of short $T_2 \cdot A_2$ and $T_3 \cdot A_3$ tracts, the most reactive thymines proved to be 3′-terminal residues of T_2 and T_3 runs located in 5′TA3′ (–2,–6,–10,–12,–16,–19,–23,–27 and –37) and 5′TG3′ (–34, +3) steps, and, in particular, T-10 of the canonical promoter –10 region hexamer TATAAT. Corresponding rate constants of oxidation varied in the range of 0.03–0.09 $M^{-1} s^{-1}$ and were larger by a factor of 2–4 than those for the 5′-adjacent thymines in T_2 runs, while the 5′-terminal bases in T_3 runs exhibited comparable or somewhat weaker reactivity than those located centrally.

It has been observed previously [3] that thymines at the 3′-end of T_n (n = 4 or 5) runs in dsDNA are highly susceptible to MnO_4^- attack, and was interpreted in terms of the particular structure of $A_n \cdot T_n$ tracts bending the helical axis of B-DNA. Our data indicate, however, that location in the 5′TA3′ step is sufficient for such a high reactivity. Inspection of the footprints reproduced in the work referred to above shows that some thymines located in isolated 5′TA3′ steps were also highly reactive. Contrary to sequence-dependent reactivity of thymines in dsDNA, in long T_n streches of single-stranded DNA domains, displaced from duplex DNA by a polyamide nucleic acid analogue, all bases exhibited similar permanganate reactivity [6, 7].

In the b3 fragment, made of both AT and GC pairs, Ts in 5′TC3′ and 5′TG3′ steps, both isolated (e.g. +48,+45,+41, +36, +21 and +14) and included in TTC and TTG sequences (+36, +28, +8), exhibited high reactivity, similarly as their counterparts in 5′TA3′ steps (between 0.005 and 0.01 $M^{-1}s^{-1}$). Particularly reactive proved to be T+14 located in 5′TC3′ step at the center of a short palindromic $(GGCC)_2$ sequence (cf. Fig. 3a); the corresponding k_j was found 3–4 times larger than for other Ts in this fragment. Extrusion from supercoiled DNA duplex of a short hairpin structure with unpaired A(+13) and T(+14) may explain high reactivity of this base. Indeed, facile oxidation by $KMnO_4$ of a single thymine in the middle of the triplet repeat region of ss$(CTG)_{15}$ DNA has been observed and documented as due to formation by this oligonucleotide of a hairpin structure [14]. In-

spection of the $KMnO_4$ footprints of various fragments of pDPL6 plasmid dsDNA [3] shows that also in this case the reactivity of Ts in 5′TC3′ steps was distinctly higher than that of 5′-adjacent bases in short T_n runs.

previously [3] that all Cs except the 3′-terminal cytosine located in short G_nC_n (n = 3, 4) tracts, react more significantly with potassium permanganate. This observation apparently does not apply to two-cytosine repeats.

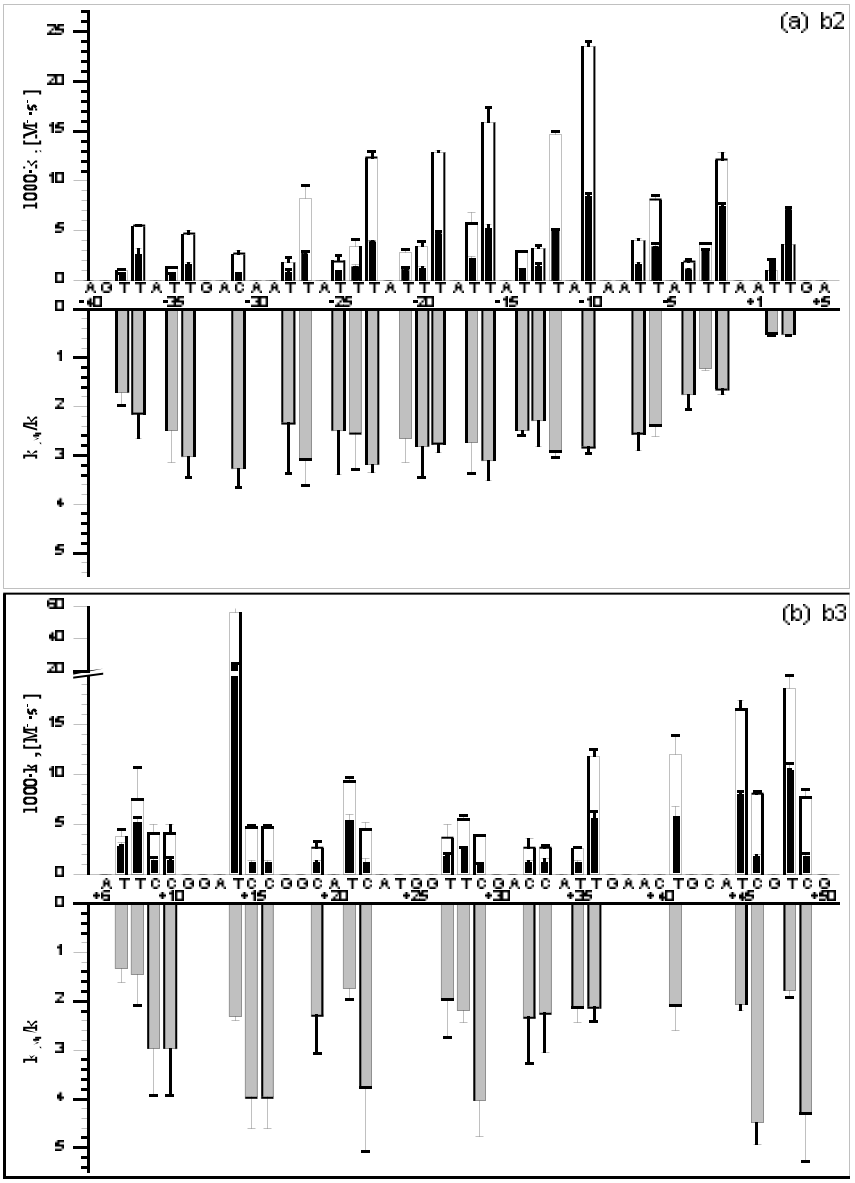

Figure 3. Column plots of k_j (black), and $k_{j,Mg}$ (white) rate constants of oxidation and of $k_{j,Mg}/k_j$ ratio (gray) for the indicated pyrimidine residues in b2 and b3 fragments of pDS3 plasmid dsDNA, panels (a) and (b), respectively.

Reactivity of cytosines was found almost independent of the nature of the 3′- and 5′-adjacent bases, including 5′CC3′ steps, and generally much lower than that of thymines; in the 5′TC3′ steps it was 3–5 times lower than that of 5′-adjacent T (cf. Fig. 3b). It has been noted

In this connection, it is worth to note that free cytidine was reported to be by far less reactive than thymidine [1, 2].

One of the objectives of this work was to determine the difference in reactivity of pyrimidines in double- and single-stranded DNA in

the melted region of the open transcriptional complex. For this purpose, we compared the rate constants of oxidation of Ts located between positions –4 and +3 of nontemplate strand of the Pa promoter in dsDNA and in the bubble region of the open complex [9], determined under similar salt and temperature conditions. It is clear from inspection of the data in Table 1 that the reactivity of corresponding Ts in the dsDNA form is by 2–3 orders of magnitude smaller as compared with that in the ssDNA form within the melted region of the transcription open complex.

barriers, as well as for longer (n = 4–6) tracts, deduced from ^{1}H NMR exchange times of adenine imino protons [19–22]. In general, A·T pairs at the 3′-end of such tracts are characterized by significantly shorter lifetimes and lower activation enthalpies and entropies than those of the successive pairs located closer to the 5′-end. Also the opening rates of A·T pairs in the TATA box have been reported to be faster by a factor of 2–3 compared to those of the AATT sequence [21]. Faster exchange rates of guanine imino protons have been also found for the TGTG box

Table 1. Comparison of $KMnO_4$ reactivity pseudo-first order rate constants for indicated thymines within nontemplate strand of Pa promoter in dsDNA (this work) and in the open complex with *Escherichia coli* RNA polymerase, in the absence of $MgCl_2$ [9]

Thymine	k_j [$M^{-1}s^{-1}$]		Ratio
	dsDNA	Open complex	
T+3	0.008	1.83	229
T+2	0.002	0.75	375
T–2	0.0077	1.97	256
T–3	0.003	4.2	1400
T–4	0.001	1.24	1240

To rationalize the high reactivity of Ts in 5′TA3′ steps it should be recalled that the TA:TA step in B-DNA is characterized by a broad major groove [15] wherefrom the 5,6 double bond of T can be attacked by MnO_4^-, has the largest twist angle among all the other dinucleotide steps in B-DNA [16], a highly flexible conformation [17] and the lowest free energy contributed to the thermodynamic stability of B-DNA [18]. Thus, the high reactivity of 5′T can be easily explained by the unique structural and thermodynamic properties of the step it belongs to. Since the GA:TC step is also characterized by a large twist angle and flexible conformation [16], the high reactivity of thymines located therein can be explained by a similar token. Furthermore, the $KMnO_4$ reactivity patterns in T_2 and T_3 tracts resemble closely those for corresponding A·T base pair opening rates and their activation energy

[23]. Theoretical molecular modeling of the pathway for the swinging out of a thymine to an open state within a B-DNA duplex has demonstrated [24] that this process requires an activation energy similar to that determined experimentally and is energetically coupled to and followed by DNA bending, which might well account for the DNA distortions underlying the measured exchange rate for the protons in duplex DNA and chemical reactivity of sterically hindered base sites. It is thus likely that such a pathway for base pair opening is also involved in permanganate oxidation of pyrimidines in dsDNA.

The magnitude of the positive effect of Mg^{2+} ions on permanganate reactivity of pyrimidines in dsDNA, measured as the ratio $k_{j,Mg}/k_j$ (cf. Fig. 3), proved to be: (i) equal to approx. 4 for cytosines in most 5′TC3′ steps and larger by a factor of approx. 2 than for

5′-adjacent thymines, (ii) similar for both Cs in 5′TCC3′ sequences, (iii) two-fold smaller for Cs in 5′CA3′ steps, (iv) comparable for thymines in 5′TC3′ and 5′TA3′ steps, but somewhat larger (by approx. 20–30%) for those in the latter steps than for preceding thymines in TTA and TTTA sequences. In one region of the Pa promoter sequence, i.e. A(–5)...G(+4), the influence of Mg^{2+} appeared distinctly lower ($k_{j,Mg}/k_j$ values for Ts at –4, –3 and –2 position are in the range of 1.1–1.5) or even negative for thymines T+3 and T+2, i.e. $k_{j,Mg}/k_j \approx 0.5$. We shall return later to this observation. The most important of the (i)–(iv) observations are certainly those indicating that Mg^{2+} ions bind to dsDNA in solution in a sequence-specific manner with a preference for TC:GA and CC:GG steps.

Rationalization of the large enhancement of the rate of oxidation of pyrimidines in dsDNA by Mg^{2+} ions should be sought, of course, within the contest of the present knowledge on the interaction of these counterions with DNA polyanion. It is believed that magnesium interacts with DNA *via* two distinct modes, the predominant diffuse binding, involving long-range electrostatic interactions between the polyanion and the surrounding counterion atmosphere, and the site binding, resulting from trapping of diffusely bound cations in negative electrostatic potential wells created by the sequence-dependent irregular shape of the molecular surface (cf. [25] and ref. cited). In mixed salt solutions, competitive interactions and counterion exchange processes affect distribution of Mg^{2+} in the vicinity of DNA [25, 26]. Experimental and theoretically calculated cation competition coefficients indicate that affinity of Mg^{2+} to DNA is by two orders of magnitude higher than that of either K^+ or Na^+ [26]. Therefore, the number of Mg^{2+} ions bound to DNA per phosphate group charge, ν_{Mg}, even at a high excess of monovalent cations can be relatively high. Indeed, under the salt conditions used in the present study, viz. 10 mM $MgCl_2$ and 100 mM KCl, $\nu_{Mg} \approx 0.3$ can be estimated according to [25] from magnesium-binding isotherms for linear polynucleotides.

Preferential diffusive interactions of hydrated magnesium ions, $Mg(OH_2)_6^{2+}$, with DNA phosphates *via* outer-sphere complexes, in accord with the Manning's counterion condensation theory [27], is well documented by numerous solution studies, e.g. by Raman spectroscopy (cf. [28, 29] and papers cited), gel electrophoresis [30], ultrasonic velocity measurements [31], and molecular dynamics modeling [32]. However, experimental evidence for sequence-dependent binding of magnesium ions in solution, involving both DNA phosphates and bases, is still indirect and scanty (cf. [22] and ref. cited, and [31, 32]). Direct evidence for the occurrence of these interactions is now emerging from analysis of high resolution X-ray crystal structures of Mg^{2+} salts of model B-DNA oligomers. It has been demonstrated that $Mg(OH_2)_6^{2+}$ cations interact with π-electron system of cytosines as well as with N7 and O6 electron-donor groups of guanine [33], and are preferentially coordinated in the minor groove by bridging phosphate groups from opposite strands thus causing further contraction of the groove at one border of the A-tract [34–36]. The strongest support to sequence-specific binding of Mg^{2+} and Ca^{2+} to DNA comes from the recent analysis of high resolution (1 Å) crystal structures of four B-DNA decamer complexes and 24 other B-DNA oligomers [37], which showed that binding of these ions to the minor and major grooves is sequence-specific. In the minor groove, it involves H-bond interactions between cross-strand DNA base atoms of adjacent base pairs and cations' water ligands, with the affinity for Mg^{2+} decreasing in the order G–G > A–G > A–C; in the major groove, cations' water ligands form H-bonds with N and O atoms from either a single base or two adjacent bases, with the affinity for Mg^{2+} in the order G–G > A–G > G–T.

The effects of Mg^{2+} on the kinetics of oxidation of pyrimidines, observed in this study, which are distinctly larger for Cs in 5′GC3′

and 5′GCC3′ sequences than that on the kinetics of Ts oxidation in 5′TA3′ and 5′TC3′ steps, being as well somewhat larger for Ts in the 5′TA3′ steps than for their 5′-adjacent neigbours in TTT and TTT runs, are much in line with the conclusions drawn from analysis of crystallographic data. Thus they provide novel evidence for the occurrence of base-specific and sequence-dependent interactions of Mg^{2+} with dsDNA also in aqueous solution.

Screening of negatively charged phosphates in B-DNA by diffusely and specifically complexed Mg^{2+} can be expected to increase local concentration of MnO_4^- anions in proximity of pyrimidine 5,6 double bonds. It can be thus safely concluded that the observed effect of Mg^{2+} on the rate of oxidation of pyrimidines in pDS3 plasmid DNA is largely electrostatic in nature.

There is also growing evidence that monovalent cations, interacting with B-DNA electrostatically and non-specifically, exhibit preferential binding to the minor groove of A-tracts [38–41], more pronounced in A_3T_3 than in T_3A_3 sequences [41]. The stronger stabilizing effect of potassium ions exerted on the conformation of A_3T_3 fragments may thus contribute to the low $KMnO_4$ reactivity of Ts in such short A-tracts, observed at 100 mM KCl in the absence of magnesium (cf. Fig. 3a).

Conformation of supercoiled DNA, like the pDS3 here studied, depends strongly on ionic conditions governing both electrostatic repulsion between phosphate charges within the double helix and between segments of the interwound superhelix [42, 43]. It has been shown that the effective diameter of 7 kb pAB4 plasmid DNA of about 5 nm in 100 mM NaCl solution strongly decreases upon addition of $MgCl_2$ to 2.9 nm at 20 mM concentration of the latter, this decrease being accompanied by a decrease of the helical repeat by about 0.05 and an increase in the negative superhelical density by approx. 0.006 [43]. At 10 mM $MgCl_2$, somewhat smaller changes (by approx. 10 per cent) of these parameters can be inferred from the presented data. Similar changes in conformation of 4 kb pDS3 plasmid DNA in 100 mM KCl solution can be expected to occur upon addition of $MgCl_2$ to 10 mM concentration. Therefore, the observed effect of Mg^{2+} on reactivity of pyrimidines in pDS3 DNA may in part be connected with the appearance of a more compact plectonemic conformation. In some regions of the superhelix a higher sterical barrier to diffusion of MnO_4^- anions may thus appear, which would result as an apparently negative effect of Mg^{2+} observed for kinetics of oxidation of T+2 and T+3 (see infra). Comparative studies on oxidizability of Ts in this region in superhelical and linear forms of B-DNA might help to verify the validity of these suggestions.

The data points at x = 2 Ms and higher permanganate doses (not shown) fall down from the fitted line (cf. Fig. 2) as if oxidizability of DNA decreased with appearance of multiple-hit lesions. An upper number of oxidized pyrimidines per whole pDS3 plasmid molecule at x = 2 Ms can be estimated, using the measured rate constants of oxidation of pyrimidines in dsDNA fragments considered (cf. Fig. 3), as about 30 and 70 in the absence of magnesium and at 10 mM $MgCl_2$, respectively. Structural and thermal melting studies on a model dsDNA containing a single thymine glycol residue instead of thymine [44, 45] have shown that the presence of thymine glycol induces (i) a significant, localized structural change in which the modified base adopts an extrahelical position and introduces a kink to the host duplex, and (ii) lowering of the thermal stability of DNA. Accumulation of such oxidation products in some DNA regions rich in reactive Ts can be expected to lead to branching and compacting of plasmid DNA, and, in turn, to a lower accessibility of some pyrimidines to the oxidant.

REFERENCES

1. Hayatsu, H. & Ukita, T. (1967) The selective degradation of pyrimidines in nucleic acids by

permanganate oxidation. *Biochem. Biophys. Res. Commun.* **29**, 556–561.

2. Iida, S. & Hayatsu, H. (1971) The permanganate oxidation of deoxyribonucleic acid. *Biochim. Biophys. Acta* **240**, 370–375.

3. McCarthy, J.G., Williams, L.D. & Rich, A. (1990) Chemical reactivity of potassium permanganate and diethyl pyrocarbonate with B DNA: Specific reactivity with short A-tracts. *Biochemistry* **29**, 6071–6081.

4. Jeppsen, C. & Nielsen, P.E. (1988) Detection of intercalation-induced changes in DNA structure by reaction with diethyl pyrocarbonate and potassium permanganate. *FEBS Lett.* **231**, 172–176.

5. Sasse-Dwight, S. & Gralla, J.D. (1991) Footprinting of protein-DNA complexes *in vivo*. *Methods Enzymol.* **208**, 146–168.

6. Nielsen, P.E., Egholm, M., Berg, R.H. & Buchardt, O. (1991) Sequence-selective recognition of DNA by strand displacement with a thymine-substituted polyamide. *Science* **254**, 1497–1500.

7. Nielsen, P.E., Egholm, M. & Buchardt, O. (1994) Evidence for (PNA)2/DNA triplex structure upon binding of PNA to dsDNA by strand displacement. *J. Mol. Recognit.* **7**, 165–170.

8. Sasse-Dwight, S. & Gralla, J.D. (1989) $KMnO_4$ as a probe for lac promoter DNA melting and mechanism *in vivo*. *J. Biol. Chem.* **264**, 8074–8081.

9. Łoziński, T. & Wierzchowski, K.L. (2001) Mg^{2+} ions do not induce expansion of the melted DNA region in the open complex formed by *Escherichia coli* RNA polymerase at a cognate synthetic Pa promoter. A quantitative $KMnO_4$ footprinting study. *Acta Biochim. Polon.* **48**, 495–510.

10. Łoziński, T., Markiewicz, W.T., Wyrzykiewicz, T.K. & Wierzchowski, K.L. (1989) Effect of the sequence-dependent structure of the 17 bp AT spacer on the strength of consensus-like *E. coli* promoters *in vivo*. *Nucleic Acids Res.* **17**, 3855–3863.

11. Łoziński, T., Adrych-Ro¿ek, K., Markiewicz, W.T. & Wierzchowski, K.L. (1991) Effect of DNA bending in various regions of a consensus-like *Escherichia coli* promoter on its strength *in vivo* and structure of the open complex *in vitro*. *Nucleic Acids Res.* **19**, 2947–2953.

12. Ide, H., Kow, Y.W. & Wallace, S.S. (1985) Thymine glycols and urea residues in M13 DNA constitute replicative blocks *in vitro*. *Nucleic Acids Res.* **13**, 8035–8052.

13. Tsodikov, O.V., Craig, M.L., Saecker, R.M. & Record, Jr., M.T. (1998) Quantitative analysis of multiple-hit footprinting studies to characterize DNA conformation changes in protein-DNA complexes: Application to DNA opening by $E\sigma^{70}$ RNA polymerase. *J. Mol. Biol.* **283**, 757–769.

14. Mitas, M.Yu.A., Dill, J., Kamp, T.J., Chambers, E.J. & Haworth, I.S. (1995) Hairpin properties of single stranded DNA containing a GC-rich triplet repeat: $(CTG)_{15}$. *Nucleic Acids Res.* **23**, 1050–1059.

15. Boutonnet, N., Hui, X. & Zakrzewska, K. (1993) Looking into the grooves of DNA. *Biopolymers* **33**, 479–490.

16. Gorin, A.A., Zhurkin, V.B. & Olson, W. (1995) B-DNA twisting correlates with base-pair morphology. *J. Mol. Biol.* **247**, 34–48.

17. Zakrzewska, K. (1992) Static and dynamic properties of AT sequences. *J. Biomol. Struct. Dynam.* **9**, 681–693.

18. Breslauer, K.J., Frank, R., Blöcker, H. & Marky, L.A. (1986) Predicting DNA duplex stability from the base sequence. *Proc. Natl. Acad. Sci. U.S.A.* **83**, 3746–3750.

19. Leroy, J.L., Charretier, E., Kochoyan, M. & Gueron, M. (1988) Evidence from base-pair kinetics for two types of adenine tract structures

in solution: Their relation to DNA structure. *Biochemistry* **27**, 8894–8898.

20. Patel, D.J. & Kozlowski, S.A. (1985) Conformation, dynamics, and structural transitions of the TATA box region of self-complementary d[(C-G)$_n$- T-A-T-A-(C-G)$_n$] duplexes in solution. *Biochemistry* **24**, 926–935.

21. Patel, D.J. & Kozlowski, S.A. (1985) Conformation and dynamics of the Pribnow box region of the self-complementary d(C-G-A-T-T-A-T-A-A-T-C-G) duplex in solution. *Biochemistry* **24**, 936–944.

22. Moe, J.G., Folta-Stogniew, E. & Russu, I.M. (1995) Energetics of base pair opening in a DNA dodecamer containing an A_3T_3 tract. *Nucleic Acids Res.* **23**, 1984–1989.

23. Lu, P., Cheung, S. & Arndt, K. (1983) Possible molecular determinants in the DNA structure of regulatory sequences. *J. Biomol. Struct. Dyn.* **1**, 509–521.

24. Ramstein, J. & Lavery, R. (1988) Energetic coupling between DNA bending and base pair opening. *Proc. Natl. Acad. Sci. U.S.A.* **85**, 7231–7235.

25. Misra, V.K. & Draper, D.E. (1999) The interpretation of Mg^{2+} binding isotherms for nucleic acids using Poisson-Boltzmann theory. *J. Mol. Biol.* **294**, 1135–1147.

26. Paulsen, M.D., Andersen, C.F. & Record, Jr., M.T. (1988) Counterion exchange reactions on DNA: Monte Carlo and Poisson-Boltzmann analysis. *Biopolymers* **27**, 1249–1265.

27. Manning, G.S. (1978) The molecular theory of polyelectrolyte solutions with applications to electrostatic properties of polynucleotides. *Q. Rev. Biophys.* **11**, 179–246.

28. Duguid, J., Bloomfield, V.A., Benevides, J. & Thomas, Jr., G.J. (1993) Raman spectroscopy of DNA-metal complexes. I. Interactions and conformational effects of the divalent cations: Mg, Ca, Sr, Ba, Mn, Co, Ni, Cu, Pd and Cd. *Biophysical J.* **65**, 1916–1928.

29. Duguid, J., Bloomfield, V.A., Benevides, J. & Thomas, Jr., G.J. (1995) Raman spectroscopy of DNA-metal complexes: II. The thermal denaturation of DNA in the presence of Sr^{2+}, Ba^{2+}, Mg^{2+}, Ca^{2+}, Mn^{2+}, Co^{2+}, Ni^{2+} and Cd^{2+}. *Biophysical J.* **69**, 2623–2641.

30. Li, A.Z., Huang, H., Re, X., Qi, L.J. & Marx, K.A. (1998) A gel electrophoretic study of the competitive effects of monovalent counterion on the extent of divalent counterions binding to DNA. *Biophys. J.* **74**, 964–973.

31. Buckin, V.A., Kankiya, B.I., Rentzeperis, D. & Marky, L.A. (1994) Mg^{2+} recognizes the sequence of DNA through its hydration shell. *J. Am. Chem. Soc.* **116**, 9423–9429.

32. MacKerell, A.D. (1997) Influence of magnesium ions on duplex DNA structural, dynamic, and solvation properties. *J. Phys. Chem.* B, **101**, 646–650.

33. Brukner, I., Susic, S., Dlakic, M., Savic, A. & Pongor, S. (1994) Physiological concentration of magnesium ions induces a strong macroscopic curvature in GGGCCC-containing DNA. *J. Mol. Biol.* **236**, 26–32.

34. McFail-Isom, L., Shui, X. & Williams, L.D. (1998) Divalent cations stabilize unstacked conformations of DNA and RNA by interacting with base π systems. *Biochemistry* **37**, 17105–17111.

35. Sines, C.C., McFail-Isom, L., Howerton, S.B., VanDerveer, D. & Williams, L.D. (2000) Cations mediate B-DNA conformational heterogenity. *J. Am. Chem. Soc.* **122**, 11048–11056.

36. Minasov, G., Tereshko, V. & Egli, M. (1999) Atomic-resolution structures of B-DNA reveal specific influences of divalent metal ions on conformation and packing. *J. Mol. Biol.* **291**, 83–99.

37. Chiu, T.K. & Dickerson, R.E. (2000) 1 Å crystal structures of B-DNA reveal sequence-specific binding and groove-specific bending of DNA by magnesium and calcium. *J. Mol. Biol.* **301**, 915–945.

38. Halle, B. & Denisov, V.P. (1998) Water and monovalent ions in the minor groove of B-DNA oligonucleotides as seen by NMR. *Biopolymers, Nucl. Acid Sci.* **48**, 210–233.

39. Denisov, V.P. & Halle, B. (2000) Sequence-specific binding of counterions to B-DNA. *Proc. Natl. Acad. Sci. U.S.A.* **97**, 629–633.

40. Hammelberg, D., McFail-Isom, L., Williams, L.D. & Wilson, W.D. (2000) Flexible structure of DNA: Ion dependence of minor-groove structure and dynamics. *J. Am. Chem. Soc.* **122**, 10513–10520.

41. Stellwagen, N.C., Magnusdottir, S., Gelfi, C. & Righetti, P.G. (2001) Preferential counterion binding to A–T tract DNA oligomers. *J. Mol. Biol.* **305**, 1025–1033.

42. Rybenkov, V.V., Vologodskii, A.V. & Cozzarelli, N.R. (1997) The effect of ionic conditions on DNA helical repeat, effective diameter and free energy of supercoiling. *Nucleic Acids Res.* **25**, 1412–1418.

43. Rybenkov, V.V., Vologodskii, A.V. & Cozzarelli, N.R. (1997) The effect of ionic conditions on the conformations of supercoiled DNA. I. Sedimentation analysis. *J. Mol. Biol.* **267**, 299–311.

44. Kao, J.Y., Goljer, I., Phan, T.A. & Bolton, P.H. (1993) Characterization of the effects of a thymine glycol residue on the structure, dynamics, and stability of duplex DNA by NMR. *J. Biol. Chem.* **268**, 17787–17793.

45. Kung, H.C. & Bolton, P.H. (1997) Structure of duplex DNA containing a thymine glycol residue in solution. *J. Biol. Chem.* **272**, 9227–9236.